

Probabilistic Assessment of Ice Rose Diagrams for Ice Drift in the Beaufort Sea

Chana Sinsabvarodom¹, Wei Chai¹, Bernt J. Leira¹, Knut V. Høyland², Arvid Naess^{3,4}

¹Department of Marine Technology, Norwegian University of Science and Technology, Trondheim, Norway

²Sustainable Arctic Marine and Coastal Technology (SAMCoT), Centre for Research-based Innovation (CRI), Norwegian University of Science and Technology

³Centre for Ships and Ocean Structures, Norwegian University of Science and Technology, Trondheim, Norway

⁴Department of Mathematical Sciences, Norwegian University of Science and Technology, Trondheim, Norway

ABSTRACT

The intention of this paper is to introduce the ice rose diagram, which is a graphical tool that makes it possible to display the ice drift speed, the occurrence frequency, and the drift direction at a particular location for a given observation period. The ice drift data is obtained from subsurface local measurements with an acoustic Doppler current profiler (ADCP) which forms the basis for construction of the ice rose diagram. The data is collected during different years from 2010 to 2017 by ADCP instruments, which are installed by means of mooring buoys in the Beaufort Sea. Probabilistic models are introduced in order to fit the data for ice drift speed and drift direction. It is found that the sea ice in the Beaufort Sea tends to drift with different speeds during the winter (i.e. the growth season) versus during the summer (i.e. the melting season). The drift speed is generally lowest during the growth season and highest during the melt season. The Weibull probability model provides the most appropriate fit for the data of ice drift speed during the growth season. For the melting season, a mixed distribution provides the best fit for the ice drift speed. Regarding ice drift direction, a mixture of von Mises distributions provides the most appropriate fit for both the growth and the melting seasons.

KEY WORDS: Ice rose diagram; Ice drift; ADCP measurement; Probabilistic assessment.

INTRODUCTION

In cold regions, sea ice will drift around in the ocean according to the influence of the environmental condition as determined by the surrounding atmosphere. The behaviour of the ice drift motion can be described by equations of motion according to the fundamental principles of physics. The ice drift motion is caused by external forces, which can be categorized into five components corresponding to wind stress at the air-ice interface, water stress at the water-ice interface, the Coriolis force, the pressure gradient due to tilting of the sea

surface on which the ice floats, and the stress transmitted through the sea ice (Campbell, 1965). Inherently, wind is the most dominant source of driving forces on the sea ice, and it is balanced by the ice-ocean drag and internal friction of the ice. The Coriolis acceleration is typically perpendicular to the ice motion, and the magnitude is normally smaller than the two major forces just mentioned. The other acceleration terms and the sea surface tilt are smaller but they still influence the ice drift in any direction (Leppäranta, 2011).

There are several research results that provide observations enabling the prediction of drift speed and direction (Schweiger and Zhang, 2015). The ice drift can be observed by several methods such as GPS tracking, local monitoring, satellite imaging etc. The tracking method can be applied to observe the drift trajectory of the sea ice or icebergs by installing the tracking instrument on the target sea ice or icebergs (Yulmetov et al., 2016). The local monitoring can be applied to investigate the speeds and direction of ice drift above observing station by using upward looking acoustic Doppler current profile (ADCP) (Belliveau et al., 1990). In the aerial view, the ice drift and ice concentration can be investigated by using satellite, which provides the ice data in aerial view. The data covers the large area but is not high resolution and accuracy.

The aim of this research is to illustrate application of the so-called ice rose diagram for the purpose of characterizing the site conditions in terms of ice drift speeds, percentage of ice drift events and drift direction in order to facilitate the design of offshore structures in polar regions. The number of loading events and their magnitudes for each attack angle are important in order to select a proper orientation of fixed offshore structures and for station keeping of ships and floating structures. Moreover, the ice rose diagram is also of advantage for ice management. The rose diagram was originally applied for characterization of wind velocities. Zelenko and Lisac (1994) studied statistical wind rose analysis. They found that the probability density function (PDF) of wind direction commonly has more than one peak. The results do not follow the ordinary probability density functions. Therefore, the mixed distributions should be applied. For wind velocities, the probabilistic model can be described by Weibull distribution (Wais, 2017). Furthermore, the rose diagram is also applied to represent the wave height and wave direction at particular locations in the Barents sea (Orimolade and Gudmestad, 2017). In this research, the ice data is collected by upward looking acoustic Doppler current profile (ADCP) instruments in the Beaufort Sea by Woods Hole oceanographic institution in order to establish the ice rose diagram.

LOCATION OF OBSERVATION

In order to establish the ice rose diagram, observational data from the Beaufort Gyre region in the Beaufort Sea by Woods Hole oceanographic institution (<http://www.whoi.edu>) is employed. In this paper, the ice rose diagram is introduced in order to display the data from station A whose location is shown in figure 1a, and its position is at longitude $75^{\circ} 00.156'$ N and latitude $150^{\circ} 0.0132'$ E in a water depth of 3,827 m. The observational system of moorings consists of bottom pressure recorders (BPR), Mclane moored profilers (MMP), upward looking sonars (ULS) and acoustic Doppler current profilers (ADCP) to utilise the highest efficiency of local measurements (Richard and Andrey, 2006) as shown in figure 1b. In the present study, the ADCP data is used to investigate the ice drift velocity. The two-dimensional vectors of ice drift velocity are observed to provide the probabilistic assessments of ice rose.

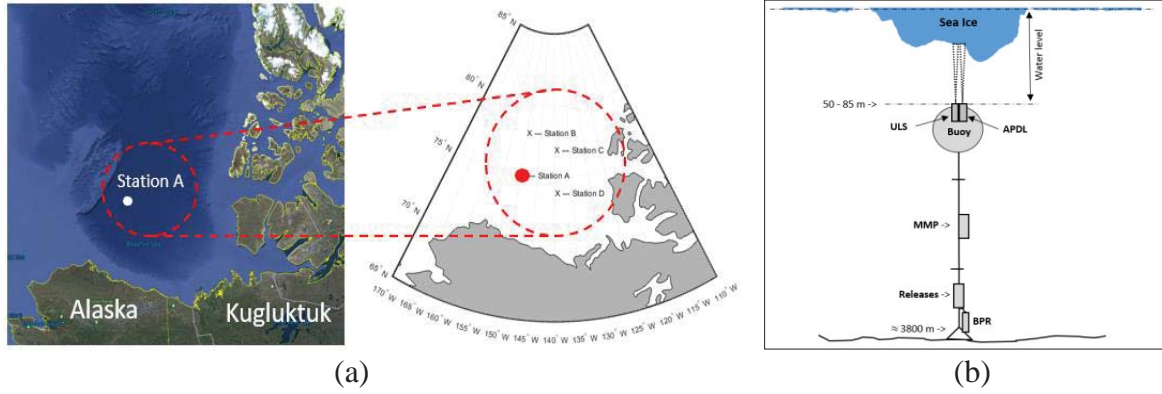


Figure 1: a) Site location for the data collected at Beaufort Gyre region in the Beaufort Sea b) Mock-up presentation of observational moorings system and the positions of the apparatus (<http://www.who.edu/website/beaufortgyre/data>)

ICE ROSE DIAGRAM

The ice drift at particular location can be represented by the ice rose diagram, which contains ice drift speeds, ice drift directions and percentage of drift even over a period. The diagram typically comprises 8-36 radiating spokes, which demonstrates ice directions in terms of the cardinal ice directions with North East South and West. A flowchart illustrating the steps associated with the construction of the ice rose diagram is given in figure 2.

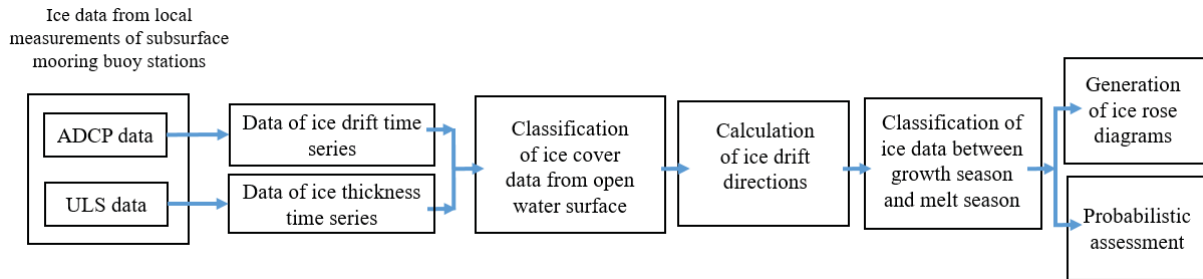


Figure 2: Flowchart of steps required for development of ice rose diagram.

THEORYICAL BACKGROUND

Horizontal Ice Drift Velocity and Direction

The ice drift velocity is obtained from ADCP measurement at every hour, t . The data consist of the velocity vectors in three dimensions. The horizontal velocity and distance of ice drift are calculated from equation 1.

$$v_{h,i}(t) = \sqrt{v_{N,i}(t) + v_{E,i}(t)} \quad (1)$$

where v_N and v_E are the hourly velocity in longitude and latitude direction, respectively. The ice drift angle θ_i is calculated from the velocity vector, $v_{N,i}$ and $v_{E,i}$ from latitude (N) and longitude (E) directions, respectively, as given in equation 2.

$$\theta_i = \arctan\left(\frac{v_{E,i}}{v_{N,i}}\right) \quad (2)$$

Correlation Coefficient

In statistic, the relation of two random variables can be determined by the correlation coefficient, ρ which indicates the positive and negative correlation by the value between [-1 , +1]. This analysis, the correlation coefficient between ice drift velocity from ADCP and ice thickness from ULS is examined as given by equation 3.

$$\rho = \frac{\sum (h_i - \bar{h}_i)(v_h - \bar{v}_h)}{\sqrt{\sum (h_i - \bar{h}_i)^2 \sum (v_h - \bar{v}_h)^2}} \quad (3)$$

where, h_i and \bar{h}_i are the ice thickness and mean value of ice thickness in each season. v_h and \bar{v}_h are the horizontal velocity and mean value of horizontal velocity in each season.

Mixed probability distributions

The nature of ice drift velocity is a complex phenomenon. The distribution of ice drift does not contain only one peak. Therefore, the probability density function, $f_{v_h}(v_h)$ of the mixture distribution is applied to cope with the multi-peak distribution. The formulation is given by equation 4.

$$f_{v_h}(v_h) = \sum_{i=1}^n w_i \cdot f_i(v_h) \quad (4)$$

where $f_i(v_h)$ denotes the individual master component distributions, w_i is the non-negative constants of mixing weights, which sum to one as given equation 5.

$$w_i > 0 \quad \text{and} \quad \sum_i^n w_i = 1. \quad (5)$$

For the two-peak distribution, the number of individual distributions in equation 4 can be set equal to two ($n = 2$). Then, the equation can be rewritten as given by equation 6.

$$f_{v_h}(v_h) = w \cdot f_1(v_h) + (1-w) \cdot f_2(v_h) \quad (6)$$

Von Mises PDF

Von Mises PDF is a continuous probability distribution of the angle with a range form 0 to 360 degrees. It is similar to the normal distribution that is located on the circular plane. The formulation of the von Mises PDF, $f_{vM}(\theta)$, is given in equation 7.

$$f_{vM}(\theta) = \frac{1}{2\pi \cdot I_0(\kappa_i)} \exp \left[\kappa_i \cos \left(\frac{\pi}{180} \cdot \theta - \mu_i \right) \right] \quad \text{for } 0^\circ \leq \theta < 360^\circ \quad (7)$$

where, $\kappa_i \geq 0$ and $0 \leq \mu_i \leq 2\pi$ are the von Mises parameters, θ is the collected values of ice drift directions, which is obtained from equation 2. $I_0(\cdot)$ is the modified Bessel function of the first kind and zero order (Carta et al., 2008).

RESULTS AND DISCUSSION

The time series from ADCP measurements in different years are plotted in figure 3. The data from mooring A is available from 2010 to 2017, except 2012-2013, which was absent. Every year, the collection of ice drift data was started at the beginning of the winter season on 1st October according to a specification of the Canadian standard.

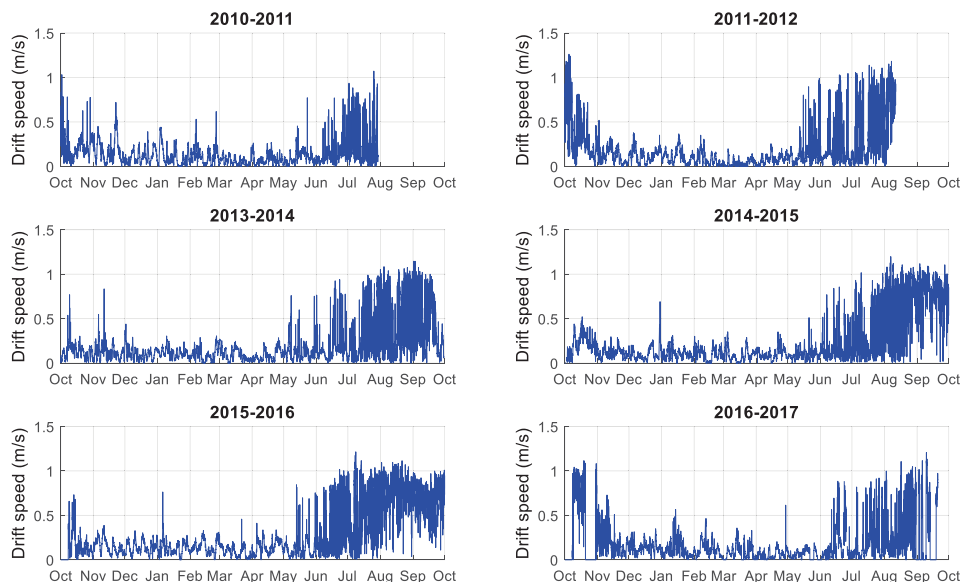


Figure 3: The horizontal velocity of ice drift from 2010 to 2017

The classification of ice cover from open waters is proceeded by elimination of the ADCP data from the time series when the ice thickness from ULS equals to zero. The example of open water detection between 2016 and 2017 is illustrated in figure 4.

The green dots represent the velocity data from ADCP measurement, which has the value of ice thickness from ULS measurement equal to zero. They are considered as the open waters data.

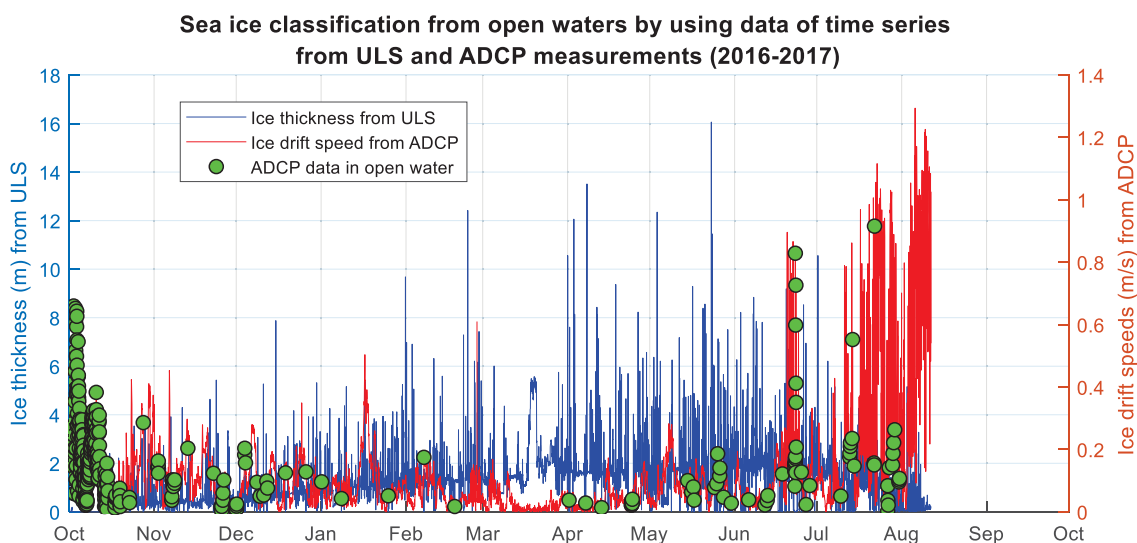


Figure 4: The example of sea ice classification from open waters by using data of time series from ULS and ADCP measurements.

We found that the sea ice drifts with different speeds during the winter and summer seasons, which can be clearly observed from the amplitude of time series from ice drift speed measurements. Sea ice drifts with the lowest speed are observed during the winter season or the growth season, approximately from October to May-June. Then, the speeds start to increase during the summer or melt season.

In connection between the ice thickness and drift speed, the ice tends to drift with a lower speed during the winter or growth season of the sea ice from November to May-June, as illustrated in figure 5, when the ice thickness is higher than 0.25-0.5 meters. It is the threshold for the reduction of ice drift speeds in growth season. The thicker ice is positively correlated with higher ice concentration in the growth season. Sea ice will induce the interaction between each other. This increases internal stress, which can be occurred sea ice deformation. Moreover, the thicker sea ice provides higher resistance, volume, mass and inertia. Whereas, in the summer or the melt season has lower ice concentration. The sea ice trends to drift with higher speeds. The decrease of ice thickness can be observed from the ULS measurements between June and September. Moreover, the scatter data of ice draft from ULS can be distinguish between the level ice and ice rubble according to the distribution of ice draft. From the data, the majority of level ice in the Beaufort seas at the observing station varies between 1.0 and 2.0 meters in June before it starts to melt. The median values of level ice thickness in each month are plotted with the range bars by 30 percent of standard deviation as shown in figure 5.

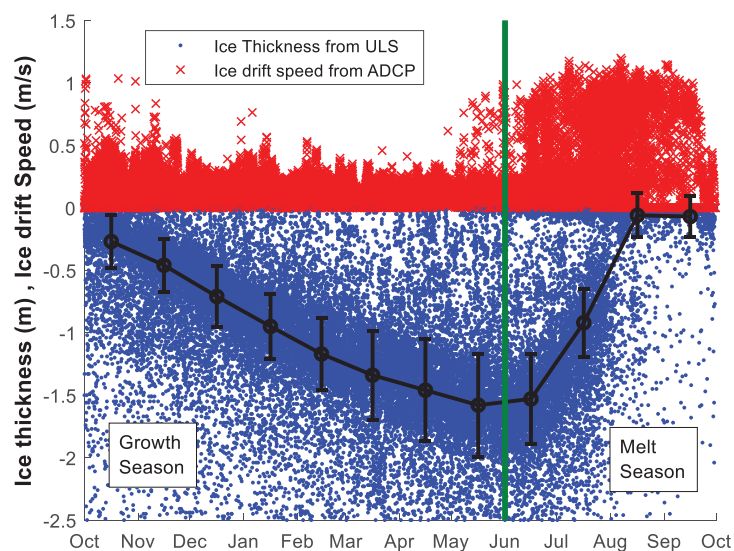


Figure 5: The observed data of ice thickness and ice drift speed based on upward looking sonar (ULS) and acoustic Doppler current profilers (ADCP) during 2010-2017.

The relationship between the ice thickness and ice drift speed is investigated by correlation coefficient according to the equation 3. As a result, the correlation coefficients in growth season and melt season from 2010-2017 have negative values, which support the hypothesis that the thicker ice drifts with lower speed. The observed data of ice thickness and ice drift speed during 2010-2017 is illustrated in figure 6a.

The values of the correlation coefficient between ice thickness and ice drift speed in the Beaufort Sea vary from -0.05 to -0.25 during the growth season. During the melting season, then the value of the correlation coefficient changes to values in the range from -0.05 to -0.48 as illustrated in figure 6b.

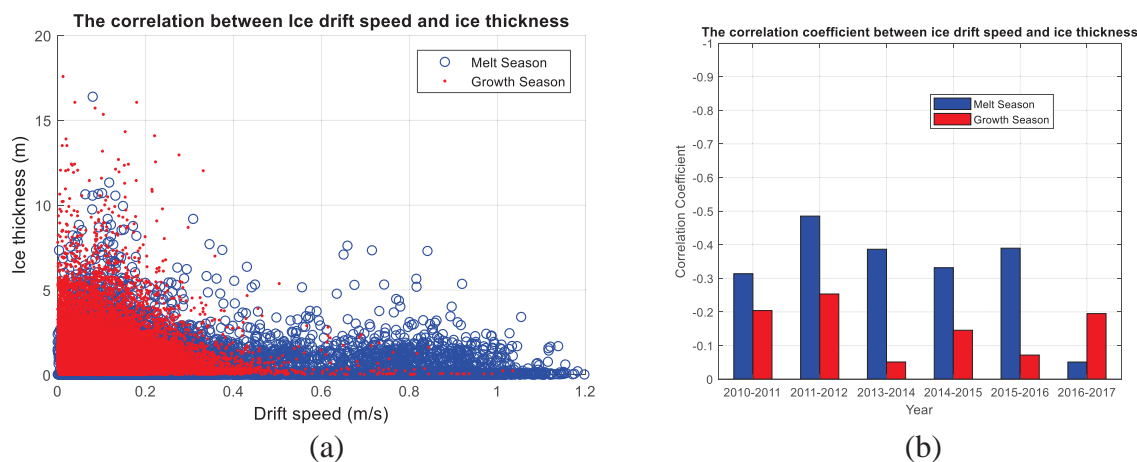


Figure 6: **a)** The observed data of ice thickness and ice drift speed based on upward looking sonar (ULS) and acoustic Doppler current profilers (ADCP) during 2010-2017. **b)** Comparison of correlation coefficients between ice thickness and ice drift speed from 2010 to 2017

The ice drift speed is inherently a stochastic process due to the randomness and time variation of the external forces imposed by the surrounding atmosphere (Leppäranta, 2011). Probabilistic models are accordingly also required in order to fit the ice drift speed and directional data as represented by the ice rose diagram for both seasons. Different types of probabilistic models have been applied as the candidates so as to fit the distribution of ice drift speed in the growth and melt season during 2010-2017. As a result, the Weibull distribution seems to provide the most appropriate fit for the present data set of the growth season. It provides the same type of the ice drift distribution, in which Weibull distribution has been used of the ice float in the Arctic sea (Yulmetov et al., 2016). The example of PDF fitting with the Weibull distribution for the accumulated data from 2010-2017 in the growth season is illustrated in figure 7a.

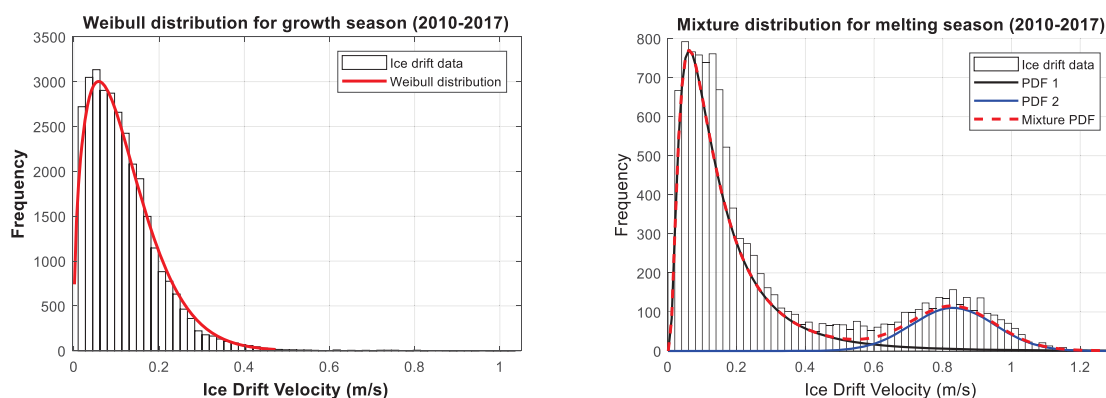


Figure 7: **a)** Fitting of a Weibull distribution for all ice drift speeds in growth season (2010-2017), **b)** Fitting of a mixed distribution for all ice drift speeds in melt season (2010-2017)

Olason and Notz (2014) also found that sea ice in the Arctic ocean drifts with the difference speeds in each month. In the present research, the empirical probability density functions of the ice drift speed during the melting season exhibited a two-peak behavior. In general, the ice drift velocities were also the highest during this season. In the present case for ice drift in melt season, the distributions will be applied by means of the mixture distributions, which are able to capture a wide variety of complex distributions (Zelenko and Lisac, 1994). An example of the fitted mixture distribution for ice drift speed in the melt season is illustrated in figure 7b.

The different years of ice drift speeds provide the different individual mixture distributions as listed in table 1.

Table 1: The individual distributions and weight factor for mixture distribution

Year	First PDF, $f_1(v_h)$	Second PDF, $f_2(v_h)$	Weight factor, w
2010 - 2011	Weibull distribution	Normal distribution	0.935
2015 - 2016	Weibull distribution	Normal distribution	0.809
2013 - 2014	Lognormal distribution	Normal distribution	0.821
2014 - 2015	Weibull distribution	Normal distribution	0.764
2015 - 2016	Lognormal distribution	Normal distribution	0.539
2016 - 2017	Lognormal distribution	Normal distribution	0.886
All	Lognormal distribution	Normal distribution	0.829

Furthermore, [Olason and Notz \(2014\)](#) also found that the trend of ice drift speed has been increasing every year since 1980. The drift speeds in growth season vary between 0 to 0.36 m/s in 2012 with mean values, which vary around 0.1 to 0.14 m/s in each month. Then, ice drift speeds increase two-three time during the melt season ([Babb, 2014](#)). According to present research, the probability density function and the cumulative distribution function based on all drift speeds from 2010 to 2017 for the growth and melting seasons are plotted in figures 8 and 9, respectively. Our analysis show that during the growth season, the lowest sea drift speeds occur. The mean values of ice drift speeds in each year are between 0.09 and 0.13 m/s in the growth seasons. The mean values of ice drift speeds increase up to the range of 0.17 to 0.46 m/s in melt seasons. Moreover, in the growth season, the sea ice has lower uncertainty of ice drift speeds than in the melt season. This can be noticed from the lower values of standard deviation and coefficient of variation (COV) as listed in table 2.

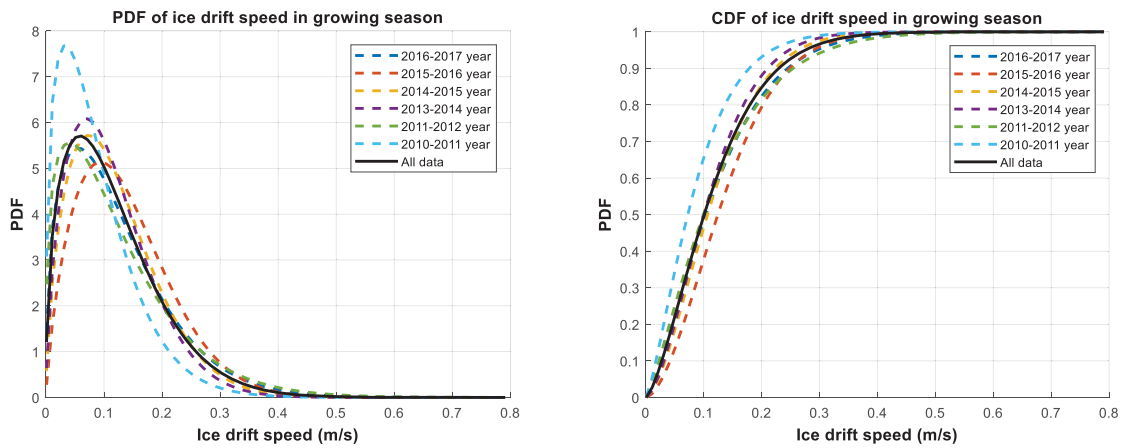


Figure 8: The PDF and CDF of ice drift speeds during the growth season from 2010-2017

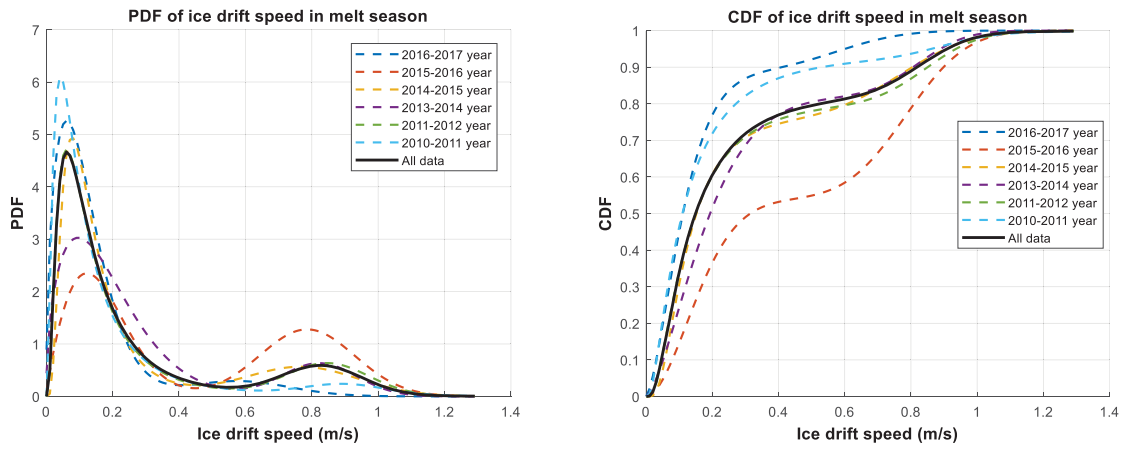


Figure 9: The PDF and CDF of drift speeds during the melting season from 2010-2017

Table 2: The statistical data of ice drift speeds [m/s]

Year	Growth Season			Melt Season		
	Mean	STD	COV	Mean	STD	COV
2010 - 2011	0.09	0.07	0.81	0.25	0.28	1.16
2015 - 2016	0.12	0.10	0.86	0.31	0.31	1.00
2013 - 2014	0.11	0.07	0.65	0.32	0.29	0.91
2014 - 2015	0.12	0.08	0.65	0.29	0.29	1.00
2015 - 2016	0.13	0.08	0.61	0.46	0.33	0.72
2016 - 2017	0.12	0.09	0.77	0.17	0.18	1.04

Regarding the direction of the drift velocity vector, the examples of fitting data for ice drift direction in growth and melt season from 2010 to 2017 are illustrated in figure 10. As a result, the ice drift direction has the highest probability between 200 and 350 degrees in the growth season, while the sea ice drifts in two major directions in the melt season within the sectors 30-120 and 250-320 degrees. Moreover, the probability density function of mixed von Mises distributions can be represented in the polar coordinate system to demonstrate the probability distribution of ice drift direction along the polar angles. The PDFs in a polar coordinate system are illustrated in figure 11.

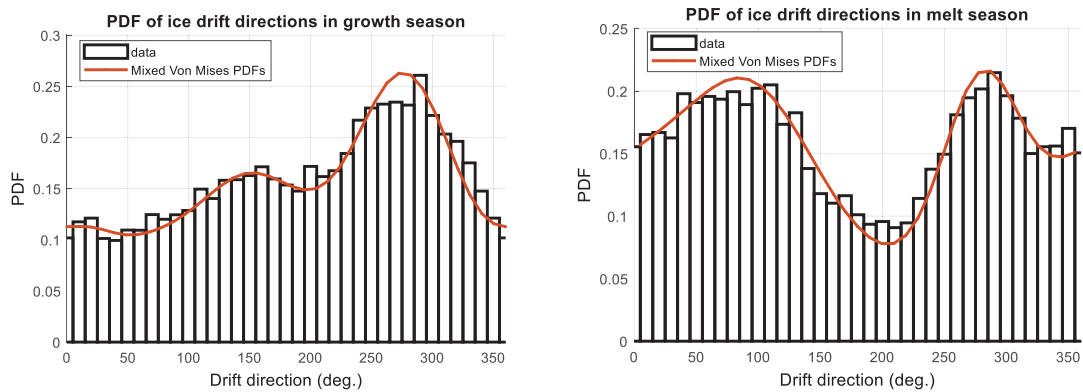


Figure 10: Examples of PDF fitting with the mixed von Mises distributions for ice drift directions in the period 2010-2017

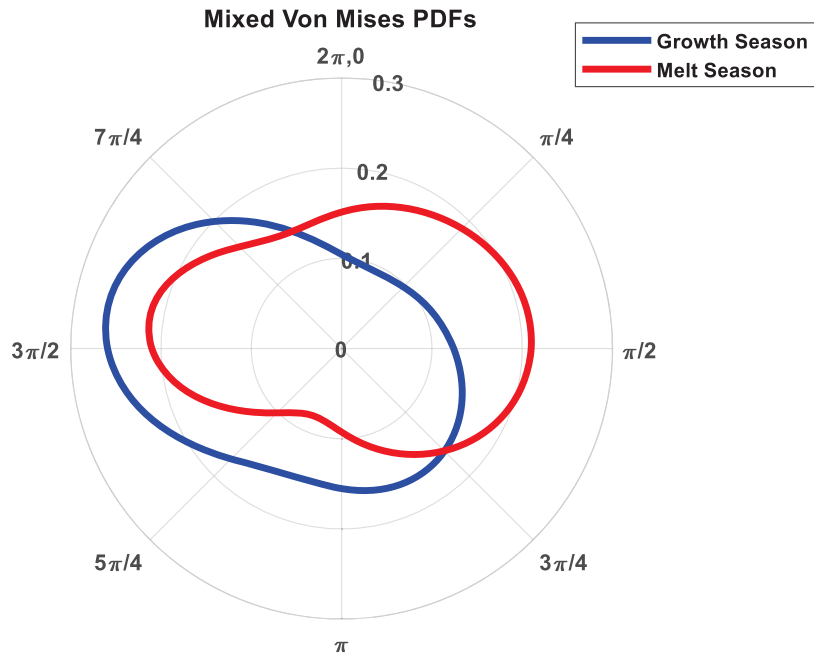


Figure 11: Mixed Von Mises PDFs of ice drift directions during the growth and melt seasons for the period 2010-2017

The ice rose diagram can be employed to display concise data for ice drift in terms of ice drift speeds, percentage of ice drift data and directional distribution for a particular location. It summarizes the ice drift data to demonstrate into one diagram. The shape of the diagram is similar to the polar distribution of the mixed Von Mises PDF. In this research, the angles of ice rose diagram are divided in every 10 degree with 36 radiating spokes. The ice rose diagrams from ADCP measurements in Beaufort Sea during growth and melt seasons from 2010 to 2017 are shown in figure 12 and 13, respectively.

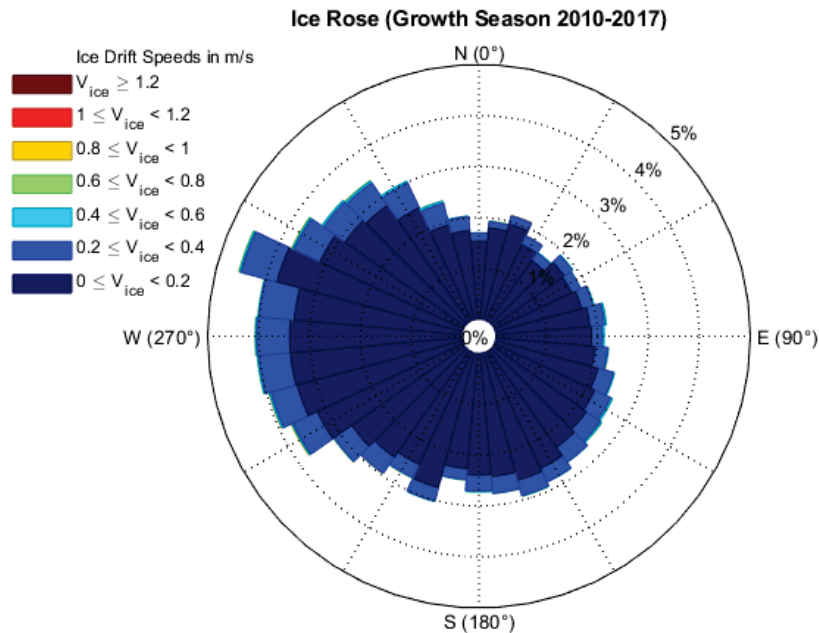


Figure 12: The ice rose diagrams from acoustic Doppler current profiler (ADCP) measurements in Beaufort Sea during the growth season

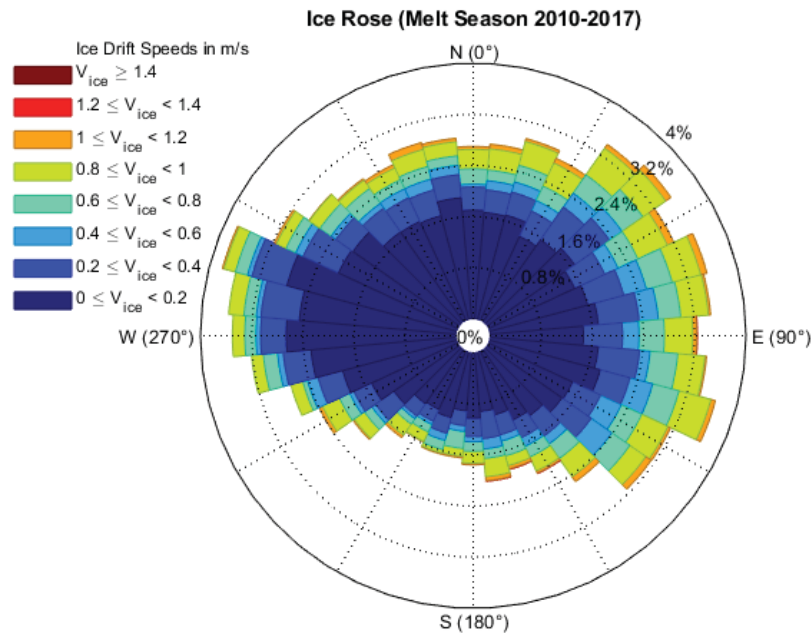


Figure 13: Ice rose diagram based on acoustic Doppler current profiler (ADCP) measurements in Beaufort Sea during melt season

CONCLUSION

The upward looking sonar (ULS) is very useful in order to classify data associated with ice cover. These ice cover data can then be applied in order to select the relevant velocity data from the acoustic Doppler current profile (ADCP) records in order to generate the ice rose diagram. The correlation coefficients between the ice thickness and ice drift speeds are generally observed to have negative values. This corresponds to thinner sea ice drifting at a higher speed than thicker ice. However, this study does not cover the iceberg.

According to the annual ice drift speeds, the sea ice in the Beaufort Sea tends to drift with lower speeds during the growth season and with a higher speed during the melting season. Weibull distribution is found to represent the most appropriate distribution for fitting of the ice drift speeds during in the growth season. During the melting season, the results of ice drift speeds demonstrate the two peak distributions. A mixed distribution was found to be best suited, which corresponds to a two-peaked distribution. Regarding ice drift directions, mixtures of von Mises distributions provides the best fit to the observing data.

The ice rose diagram provides the basic requirements of the ice drift data in the particular location or specific site location. The ice rose diagram is of particular advantage for structural design of both bottom-fixed support and floating offshore structures. Moreover, the ice rose diagram is not applicable only in the Beaufort Sea, but also it can be applied to other locations of ice cover areas.

ACKNOWLEDGMENTS

This work has been carried out within the NTNU Oceans Pilot project "*Risk, reliability and ice data in arctic marine environment*". Grants from the *Norwegian Ship-owners Association Fund at NTNU* is acknowledged. The data from ice measurements were collected and made available by the Beaufort Gyre Exploration Program based at the Woods Hole Oceanographic Institution (<http://www.whoi.edu/beaufortgyre>) in collaboration with researchers from Fisheries and Oceans Canada at the Institute of Ocean Sciences. We gratefully acknowledge their effort and

express our appreciation for making the measurement data publicly available. Moreover, the authors wish to thank Ilija Samardžija for valuable discussions in connection with ADCP measurement.

REFERENCES

- Babb, D., 2014. Sea ice motion within the Beaufort Sea. Master Thesis University of Manitoba.
- Belliveau, D., Bugden, G., Eid, B., Calnan, C., 1990. Sea ice velocity measurements by upward-looking Doppler current profilers. *Journal of Atmospheric and Oceanic Technology* 7 (4), 596-602.
- Campbell, W.J., 1965. The wind-driven circulation of ice and water in a polar ocean. *Journal of Geophysical Research* 70 (14), 3279-3301.
- Carta, J.A., Bueno, C., Ramírez, P., 2008. Statistical modelling of directional wind speeds using mixtures of von Mises distributions: Case study. *Energy Conversion and Management* 49 (5), 897-907.
- Leppäranta, M., 2011. The drift of sea ice. Springer Science & Business Media.
- Olason, E., Notz, D., 2014. Drivers of variability in Arctic sea-ice drift speed. *Journal of Geophysical Research: Oceans* 119 (9), 5755-5775.
- Orimolade, A., Gudmestad, O., 2017. On weather limitations for safe marine operations in the Barents Sea, IOP Conference Series: Materials Science and Engineering. IOP Publishing, p. 012018.
- Richard, K., Andrey, P., 2006. BGOS ULS Data Processing Procedure. Woods Hole Oceanographic Institution.
- Schweiger, A., Zhang, J., 2015. Accuracy of short-term sea ice drift forecasts using a coupled ice-ocean model.
- Wais, P., 2017. Two and three-parameter Weibull distribution in available wind power analysis. *Renewable Energy* 103, 15-29.
- Yulmetov, R., Marchenko, A., Løset, S., 2016. Iceberg and sea ice drift tracking and analysis off north-east Greenland. *Ocean Engineering* 123, 223-237.
- Zelenko, B., Lisac, I., 1994. On the statistical wind rose analysis. *Theoretical and Applied Climatology* 48 (4), 209-214.